PLOS ONE

RESEARCH ARTICLE

Cardiac Myosin Binding Protein C Phosphorylation Affects Cross-Bridge Cycle's Elementary Steps in a Site-Specific Manner

Li Wang[1,2]*, Sakthivel Sadayappan[3], Masakata Kawai[1]

1. Department of Anatomy and Cell Biology, College of Medicine, University of Iowa, Iowa City, Iowa, United States of America, **2.** School of Nursing, Soochow University, Suzhou, Jiangsu, China, **3.** Department of Cell and Molecular Physiology, Health Sciences Division, Loyola University Chicago, Maywood, Illinois, United States of America

*li-wang-1@suda.edu.cn

Citation: Wang L, Sadayappan S, Kawai M (2014) Cardiac Myosin Binding Protein C Phosphorylation Affects Cross-Bridge Cycle's Elementary Steps in a Site-Specific Manner. PLoS ONE 9(11): e113417. doi:10.1371/journal.pone.0113417

Editor: Xiaolei Xu, Mayo Clinic, United States of America

Received: July 19, 2014

Accepted: October 23, 2014

Published: November 24, 2014

Data Availability: The authors confirm that all data underlying the findings are fully available without restriction. All relevant data are within the paper.

Funding: This work was supported by grants from the National Institutes of Health HL070041 (MK), R01HL105826 and K02HL114749 (SS) (http://www.nih.gov/), The American Heart Association - Scientist Development Grant (0830311N), Grant-in-Aid (14GRNT20490025) (SS) and Grant-in-Aid (13GRNT16810043) (MK) (http://www.heart.org/HEARTORG/). The content is solely the responsibility of the authors and does not necessarily reflect the official views of the funding organizations. The funders had no role in study design, data collection and analysis, decision to publish, or preparation of the manuscript.

Competing Interests: The authors have declared that no competing interests exist.

Abstract

Based on our recent finding that cardiac myosin binding protein C (cMyBP-C) phosphorylation affects muscle contractility in a site-specific manner, we further studied the force per cross-bridge and the kinetic constants of the elementary steps in the six-state cross-bridge model in cMyBP-C mutated transgenic mice for better understanding of the influence of cMyBP-C phosphorylation on contractile functions. Papillary muscle fibres were dissected from cMyBP-C mutated mice of ADA (Ala273-Asp282-Ala302), DAD (Asp273-Ala282-Asp302), SAS (Ser273-Ala282-Ser302), and t/t (cMyBP-C null) genotypes, and the results were compared to transgenic mice expressing wide-type (WT) cMyBP-C. Sinusoidal analyses were performed with serial concentrations of ATP, phosphate (Pi), and ADP. Both t/t and DAD mutants significantly reduced active tension, force per cross-bridge, apparent rate constant ($2\pi c$), and the rate constant of cross-bridge detachment. In contrast to the weakened ATP binding and enhanced Pi and ADP release steps in t/t mice, DAD mice showed a decreased ADP release without affecting the ATP binding and the Pi release. ADA showed decreased ADP release, and slightly increased ATP binding and cross-bridge detachment steps, whereas SAS diminished the ATP binding step and accelerated the ADP release step. t/t has the broadest effects with changes in most elementary steps of the cross-bridge cycle, DAD mimics t/t to a large extent, and ADA and SAS predominantly affect the nucleotide binding steps. We conclude that the reduced tension production in DAD and t/t is the result of reduced force per cross-bridge, instead of the less number of strongly attached cross-bridges. We further conclude that cMyBP-C is an allosteric activator of myosin to increase

cross-bridge force, and its phosphorylation status modulates the force, which is regulated by variety of protein kinases.

Introduction

Muscle contraction is achieved by the cyclic interaction between myosin cross-bridges of the thick filament and actin on the thin filament, during which the actin-myosin-ATP complex undergoes several different states to achieve the transduction of chemical energy stored in ATP to mechanical work. This is called the cross-bridge cycle, and each step within the cycle is called an elementary step. A complete cross-bridge model which include six elementary steps is described in Fig. 1 (Scheme 8 in [1]). From experiments that observe the effects of ATP, phosphate (Pi), and ADP on tension transients, the kinetic constants of the elementary steps can be characterized [2].

Myosin binding protein C (MyBP-C), as an integral part of the thick filament [3], is implicated in both regulatory and structural functions in striated muscles [4]. Its cardiac isoform (cMyBP-C) can be phosphorylated at multiple sites located in the M domain between domains C1 and C2 [5,6]. The phosphorylation status of cMyBP-C is associated with various pathological conditions in the heart, and plays a critical role in regulating force generation by modulating the thick-to-thin filament interaction [6–9]. Three hierarchically accessible and functionally unequal phosphorylation sites, Ser(S)273, 282 and 302, have been identified in murine and are homologous to humans [10–13]. The pattern of phosphorylation at the three sites is not random, and has shown mutual interactions which can be positive or negative [14]. Among the three sites, S282 is phosphorylated first before phosphorylation takes place at S273 and S302 [10], hence S282 is thought to play a critical role in the phosphorylation of cMyBP-C [13].

The histological characteristics and cardiac function at the whole organ level were studied in cMyBP-C transgenic mice of ADA (Ala273-Asp282-Ala302), DAD (Asp273-Ala282-Asp302), SAS (Ser273-Ala282-Ser302), and wild-type (WT: Ser273-Ser282-Ser302) genotypes (Ala: phospho-ablation; Asp: phosphomimetic), which were created on the cMyBP-C knockout (t/t) background [13]. The Asp or Glu mutant mimics the phosphorylated state of Ser; and alanine, an amino acid that is structurally similar to Ser, is the common replacement for phospho-ablation [15]. Although the t/t phenotype can be completely rescued by WT, it can only be partially rescued by ADA, DAD and SAS [13]. Among them, mouse hearts from DAD show significant hypertrophy, fibrosis, and myocyte disarray, mimicking the t/t phenotype [13]. A recent study found that DAA and AAD mice exhibited left ventricular dilation, interstitial fibrosis, irregular cardiac rhythm, and sudden cardiac death, suggesting that the normal phosphorylation status of the three Ser residues is essential for cardiac function, and that chronic phosphorylation at one site, with the inability to phosphorylate the other sites, can be detrimental to the maintenance of normal cardiac structure and function [16].

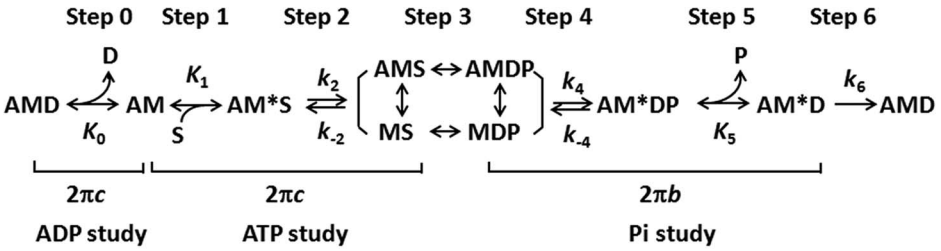

Figure 1. Elementary steps of the cross-bridge cycle in striated muscle fibers. In this scheme, force is generated at step 4 as demonstrated by experiments using rabbit psoas muscle fibers with sinusoidal analyses [22], pressure-release experiments [28], and caged Pi experiments [27]. Step 0: ADP release with the dissociation constant $1/K_0$; Step 1: ATP binding with the association constant K_1; Step 2: Cross-bridge detachment and possibly recovery stroke with the forward rate constant k_2, the reversal rate constant k_{-2}, and the equilibrium constant $K_2=k_2/k_{-2}$; Step 3: ATP cleavage followed by a formation of weakly attached/detached cross-bridges; Step 4: Pi isomerization and force generation with the forward rate constant k_4, the reversal rate constant k_{-4}, and the equilibrium constant $K_4=k_4/k_{-4}$; Step 5: Pi release with the dissociation constant $1/K_5$; Step 6: ADP isomerization and work performance (filament sliding). A=Actin, M=Myosin, D=ADP, S=ATP, and P=phosphate.

doi:10.1371/journal.pone.0113417.g001

With the importance of cMyBP-C phosphorylation in contraction, regulation, and the hierarchically functional S273, S282 and S302 sites in mind, we have recently found that phospho-aberrant (nonphosphorylatable) Ala282 combined with phosphomimetic residues Asp273 and/or Asp302 (in DAD) is detrimental to cardiomyocytes as evidenced by the lower active isometric tension and altered cross-bridge kinetics with decreased $2\pi c$ (fast rate constant) and increased $2\pi b$ (medium rate constant). On the other hand, a single change of residue 282 to phospho-aberrant Ala (SAS), or to phosphomimetic Asp together with changes of residues 273 and 302 to nonphosphorylatable Ala (ADA), caused a minute change in fibre mechanics [17]. Based on these findings, we aimed at studying further the site-specific effect of cMyBP-C phosphorylation on cross-bridge force and elementary steps of the cross-bridge cycle (Fig. 1). For this purpose, different concentrations of ATP (0.05–10 mM), Pi (0–30 mM), and ADP (0–3 mM) were applied to skinned cardiac papillary and trabecular muscle fibres. During Ca^{2+} activation, small amplitude sinusoidal length changes were applied to the fibres and the tension transients were recorded, through which the kinetic constants were deduced, and the elementary steps as well as force per cross-bridge were characterized. We found that the reduced tension production in DAD and t/t is the result of reduced force per cross-bridge, instead of the less number of strongly attached cross-bridges, emphasizing the significance of cMyBP-C in allosteric activation of cross-bridge force.

Materials and Methods

1. Animals

All the animal experiment protocols were approved by the Institutional Animal Care and Use Committees at Loyola University Chicago, conforms the contents of *Guide for the Use and Care of Laboratory Animals* published by the National

Institutes of Health. The transgenic mouse models used in the present study were in the t/t background lacking endogenous cMyBP-C, and they have been reported in our previous investigations [17]. t/t is a hypertrophic cardiomyopathy mutant mouse with C-terminal modifications that causes an absence of cMyBP-C in sarcomeres [18]. WT mice were crossed on the t/t background, and used as the control. Totally 16 mice of WT, t/t, ADA, DAD, and SAS models were tested. The details of the mouse models, the information on the number of mice used, their age and gender, can be found in Wang et al [17].

2. Muscle fibre preparations

Skinned mouse cardiac papillary and trabecular muscle fibres (strips) were prepared from both ventricles of the heart that was removed after the mice were euthanized through intraperitoneal injection of Na pentobarbital at 50 mg/kg. All efforts were made to minimize potential pain, suffering or distress. The method is same as previously described [17].

3. Experimental procedure

Experimental procedure is similar to the one in our previous study [19]. Fibres were dissected and mounted on the experimental apparatus by attaching their ends to two stainless-steel hooks with a small amount of nail polish. One hook was connected to a length driver to change the fibre length, and the other to a tension transducer to detect isometric tension and its transients. After mounting, fibres were soaked in relaxing solution for a few minutes and thereafter further skinning for 20 min in the relaxing solution to which 1% Triton X-100 was added. Before applying activating solutions for mechanical measurements, fibres were washed with the relaxing solution and their length was adjusted to remove the slack. This achieved sarcomere length of 2.1–2.2 μm, as measured by laser diffraction [20]. ATP, Pi, and/or ADP studies were performed on the fibres to determine the kinetic constants of the elementary steps based on the six-state cross-bridge model (Fig. 1). In these studies, activating solutions contain a series of concentration of ATP (S: 0.05–10 mM), Pi (P: 0–30 mM), or ADP (D: 0–3 mM). The rigor stiffness was tested in the end. The solution compositions are listed in Table 1. All experiments were performed at 20℃ and a circulating water bath system was used to maintain the constant temperature.

4. Sinusoidal analysis

Sinusoidal analysis method has been described in our previous publications [17,19]. In the current study, the mouse cardiac muscle fibres are studied at 20℃. The frequency (f) response function $Y(f)$ (complex modulus) of the tension change to the stress change is resolved into the sum of two exponential processes B and C. $2\pi b$ is the apparent rate constant of process B, called delayed tension; and $2\pi c$ is the apparent rate constant of processs C, called fast tension recovery. They are associated with the active interaction of myosin cross-bridges with actin

Table 1. Solution compositions.

Ingredient (mM)	Relaxing	ATP study		Pi study		ADP study			Rigor solution
		0S	10S	0P	30P	00D	0D	3D	
$K_2CaEGTA$	-	6	6	6	6	6	6	6	-
K_2H_2EGTA	6	-	-	-	-	-	-	-	-
Na_2H_2ATP	7	0	12.12	6.12	6.058	2.9	2.93	2.86	-
NaADP	-	-	-	-	-	-	0	11.84	-
A_2P_5	-	-	-	-	-	-	0.1	0.1	-
Na_2CP	-	15	15	15	15	15	-	-	-
HK_2PO_4+H_2KPO_4[1]	8	8	8	0	30	8	8	8	8
$MgAc_2$	2	1.69	11.54	6.68	6.44	2.83	2.75	5.67	-
NaAc	41	25	0.77	12.77	12.89	9.2	39.1	27.4	55
KAc	70.5	74	33.23	72.08	2.54	77	91.8	50.7	122
KCl	-	12	12	12	12	-	-	-	-
KOH	19	5.4	29.37	15.82	21.26	5.8	5.86	25.8	5
MOPS	10	10	10	10	10	10	10	10	10
NaN_3	-	-	-	-	-	10	10	10	-
CK (U/ml)	-	80	80	80	80	80	-	-	-

[1]Equimolar mixture.

Ac=acetate, CP=creatine phosphate, Pi=phosphate, CK=creatine kinase. Ionic strength of all solutions is 200 mM. pCa of activating solutions is 4.34–4.65, and that of relaxing solution is>9. For activating solutions, $[Mg^{2+}]$ 1 mM; $[MgATP^{2-}]$ in the ηS solution is η mM, in ηD solution is 2 mM, and in ηP solution is 5 mM; $[Na^{+}]$ 55 mM, and pH is adjusted to 7.00±0.02 by KOH. Solution 0S and 10S were mixed the by ratio (10-η):η to make the ηS solution used in the ATP study. Solution 0P and 30P were mixed the by ratio (30-η):η to make the ηP solution used in the Pi study. Similarly, solution 0D and 3D were mixed the by ratio (3-η):η to make the ηD solution used in the ADP study.

doi:10.1371/journal.pone.0113417.t001

which leads to chemomechanical energy transduction [21]. The parameters of exponential processes were studied in the present study as functions of [ATP], [Pi], and [ADP] to deduce the kinetic constants of elementary steps of the cross-bridge cycle and as reported [22]. $Y(\infty)$ is generally called "stiffness" in this report. A detailed description of the sinusoidal analysis method was published previously [21].

5. ATP study

In the ATP study, through applying different concentrations of ATP (0.05, 0.1, 0.2, 0.5, 1, 2, 5, and 10 mM) to the skinned fibres and recording tension and its transients during each activation at pCa 4.34–4.65, the exponential process C was studied aiming at observing the kinetic constants of the ATP binding step 1 (K_1), and the subsequent rapid cross-bridge detachment step 2 (k_2 and k_{-2}) (Fig. 1). The apparent rate constant $2\pi c$ was deduced from $Y(f)$ during activation at each ATP concentration. The relationship between $2\pi c$ and [ATP] were fitted to Eq. 1 which was developed based on the cross-bridge model in Fig. 1, where S represents [ATP], D represents [ADP] and D_0 represents the contaminating [ADP] in solutions and fibres. Because of the presence of creatine phosphate (CP) and creatine kinase (CK) (Table 1) in the ATP study, K_0 (D+D_0) in Eq. 1 was assumed

to be 0 as the first approximation.

$$2\pi c = \frac{K_1 S}{1 + K_0(D + D_0) + K_1 S} k_2 + k_{-2} \quad (1)$$

(Eq. 1 is based on Eq. 16 of [22].)

6. Pi study

The effect of Pi on the exponential processes B and C and isometric tension were studied through applying 0, 2, 4, 8, 16, and 30 mM Pi to the fibres, with the purpose to investigate the effects of cMyBP-C mutants on the force generation step 4 and the Pi release step 5 (Fig. 1). The sum of the two apparent rate constants ($2\pi b$+$2\pi c$) was deduced from the Pi study, and the relationships between [Pi] and ($2\pi b$+$2\pi c$), and [Pi] and tension were fitted to Eqs. 2 and 3, respectively. These equations were derived based on the cross-bridge model in (Fig. 1) [22]:

$$2\pi b + 2\pi c = Q + \frac{K_5 P}{1 + K_5 P} k_{-4} \quad (2)$$

(Eq. 2 comes from Eq. 14 of [22].)

$$Tension = T_{56}(X_5 + X_6) = \frac{K_5 P + 1}{1 + (1 + 1/K_4) K_5 P} T_{56} \quad (3)$$

(Eq. 3 is derived from Eq. 5 of [23] by setting $T_5 = T_6 = T_{56}$.)

where P represents [Pi], X_5 and X_6 represent the probabilities of cross-bridges in the AM*DP and AM*D states, respectively, and T_{56} is the tension supported by these states, i.e., the tension when all the cross-bridges are distributed either at X_5 or X_6, and it is proportional to force per cross-bridge. k_{-4} (rate constant of the reverse force generation step) and K_5 (Pi association constant) were first determined by fitting the rate constant data to Eq. 2. Then, based on this K_5, the tension data were fitted to Eq. 3 to determine K_4 (equilibrium constant of force generation step) and T_{56}. k_4 is calculated as $k_4 = K_4 k_{-4}$ in the usual way.

7. ADP study

To characterize the association constant (K_0) of ADP to cross-bridges, the effect of ADP was studied through applying 0–3 mM ADP to muscle fibres, in which [ATP] was fixed to 2 mM and [Pi] to 8 mM (Table 1). By fitting the relationship between the rate constant $2\pi c$ and [ADP] to Eq. 1, K_0 and D_0 were deduced. Here we used K_1, k_2, and k_{-2} derived from the ATP study, and S=2 mM (experimental condition). During the ADP study, 00D solution, which contained CP and CK but no A_2P_5 nor ADP, was first applied to the fibres, followed by the 0D solution, which did not contain CP, CK, or ADP, but contained A_2P_5 (adenyl kinase inhibitor). The 1D, 2D and 3D solutions were applied sequentially thereafter. These solutions enable to find out the contaminating ADP concentration (D_0) in the 0D–3D solutions by extrapolation.

8. Cross-bridge distribution

Based on Eqs. 10–13 of [24], the cross-bridge distribution at AMDP (X_{34}), AM*DP (X_5) and AM*D (X_6) states in (Fig. 1) was calculated under the activating conditions.

9. Rigor stiffness

The rigor state was induced at the end of experiments by applying the rigor solution twice, and rigor stiffness was measured at 100 Hz.

10. Myofilament proteins' phosphorylation levels

Pro-Q Diamond dye provides the capability of quantifying the protein phosphorylation levels on a proteome-wide scale through the fluorescence detection of phosphoserine-, phosphothreonine-, and phosphotyrosine-containing proteins directly in sodium dodecyl sulfate (SDS)-polyacrylamide gels and two-dimensional (2-D) gels [25]. The fluorescence signal intensity correlates with the number of phosphorylated residues on the protein [25]. The pseudophosphorylation with Glu or Asp is undetected by this method owing to the absence of phosphate. The phosphorylation levels of cMyBP-C, cardiac troponin T (cTnT), cardiac troponin I (cTnI), tropomyosin (Tm), and myosin regulatory light chain (RLC) were analyzed by Pro-Q Diamond-stained gels and normalized against SYPRO Ruby-stained total protein levels. The procedure of Pro-Q Diamond and SYPRO Ruby staining have been previously described [26]. The protein phosphorylation levels in each mouse model were expressed in a value normalized to the average level of WT. All proteins were quantified in five mouse models, including WT, t/t, ADA, DAD, and SAS, with 2–3 mice in each model.

11. Statistics

All the data were expressed as mean $\pm$ standard error (SE). One-way analysis of variance (ANOVA) was applied to determine the significance of the difference among different groups of muscle preparations, with post-hoc range tests (least significant difference, LSD) using pair wise multiple comparisons. A significant difference was defined as $^{*}0.01<P\leq0.05$, and a highly significant difference as $^{**}P\leq0.01$. A slight effect was defined as $^{(*)}$ $0.05<P\leq0.1$.

Results

1. The ATP binding and cross-bridge detachment steps (steps 1 and 2 in Fig. 1)

During Ca^{2+} activation at varied ATP concentration, isometric tension was measured, sinusoidal analysis was performed to obtain the complex modulus data $Y(f)$, and the rate constant of the exponential process C ($2\pi c$) was derived from $Y(f)$ as described previously [21]. These are plotted in Fig. 2A in the semi log scale.

$2\pi c$ increased when [ATP] was increased from 0.05 mM to 1 mM, and saturated by 10 mM (Fig. 2A). The continuous curves in Fig. 2A represent the best fit curves to Eqs. 1. This hyperbolic (sigmoid in the semi log scale) relationship between $2\pi c$ and [ATP] is a common character of skeletal and cardiac muscle fibres [19,23]. The t/t and DAD mice showed significantly decreased $2\pi c$ compared to WT. Isometric tension decreased with the increase of [ATP] as shown in (Fig. 2B). DAD had the lowest tension, followed by t/t.

Through fitting the relationship between $2\pi c$ and [ATP] to Eq. 1, the kinetic constants surrounding step 1 (K_1) and step 2 (k_2) were deduced and plotted in (Fig. 2C). Compared with WT, t/t and SAS mice showed significantly decreased ATP association constant (K_1), t/t and DAD showed significantly decreased k_2 (forward rate constant of the cross-bridge detachment step 2), whereas ADA group showed somewhat opposite effects as evidenced by the slightly increased K_1 (P=0.1) and k_2 (P=0.09) (Fig. 2C). Because $2\pi c$ extrapolated near to the origin in the linear plot of (Fig. 2A), equilibrium constant of the cross-bridge detachment step (K_2) was not calculated. This indicates that k_{-2} is very small, hence K_2 is very large.

2. The force generation and Pi release steps (steps 4 and 5 in Fig. 1)

During Ca^{2+} activation at varied Pi concentration, isometric tension was measured, sinusoidal analysis was performed to obtain Y(f), and the rate constant ($2\pi b$) of process B and the rate constant ($2\pi c$) of process C were derived. These are plotted in (Figs. 3A) ($2\pi b$+$2\pi c$) and B (tension). The continuous curves represent the best fit curves to Eqs. 2 and 3. Similar to the ATP study, both t/t and DAD mutants produced significantly smaller apparent rate constants ($2\pi b$+$2\pi c$) at 0–30P with the lowest values in t/t mice. The tension at each [Pi] was significantly less in both DAD and t/t mice ($P \leq 0.05$ in t/t and DAD except at 30P in DAD).

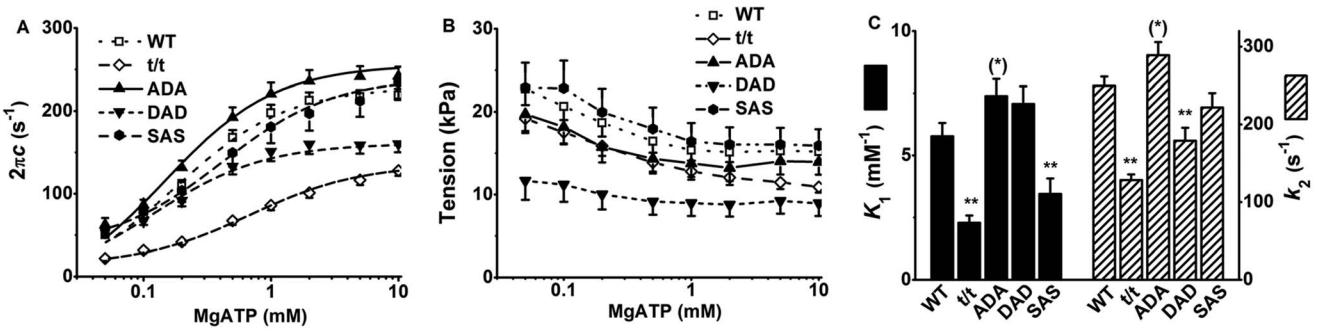

Figure 2. Results of the ATP study and parameters deduced from it. (A) Apparent rate constant $2\pi c$ versus [ATP] plot, (B) active tension versus [ATP] plot, and (C) the ATP association constant (K_1) and the forward rate constant of the cross-bridge detachment step (k_2). n=20, 34, 21, 14, and 14 for WT, t/t, ADA, DAD, and SAS mice, respectively. In (A), the continuous lines are the best fit curves to Eq. 1. $2\pi c$ was significantly smaller in t/t than in WT from 0.05S to 10S. DAD showed significantly smaller $2\pi c$ in the high concentration range of ATP (0.5S–10S). In (B), tension production in DAD mice was significantly lower than that in WT, whereas the lower tension in t/t than WT did not reach the significant level. In (C), $^{**}P \leq 0.01$, and $^{(*)}$ $0.05 < P \leq 0.1$ when compared with WT.

doi:10.1371/journal.pone.0113417.g002

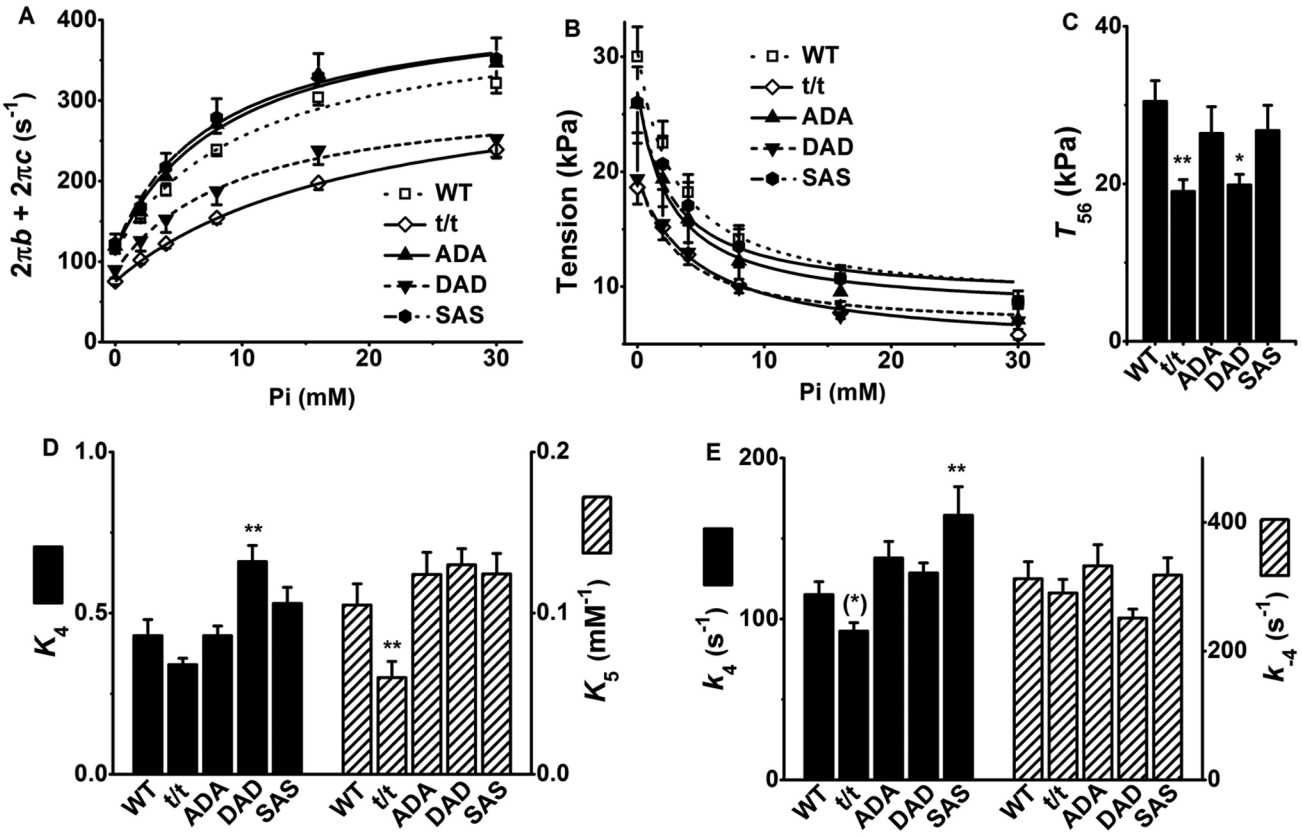

Figure 3. Results of the Pi study and parameters deduced from it. (A) Sum of the apparent rate constants ($2\pi b$+$2\pi c$) versus [Pi] plot, (B) tension versus [Pi] plot, (C) force per cross-bridge (T_{56}), (D) equilibrium constants of force generation (K_4) and Pi association (K_5), and (E) the forward (k_4) and reverse (k_{-4}) rate constants of the force generation step. n=17, 28, 13, 9, and 12 for WT, t/t, ADA, DAD and SAS mice, respectively. The continuous lines in (A) are the best fit curves to Eq. 2, and the continuous lines in (B) are the best fit curves to Eq. 3. **$P\leq0.01$, *$0.01<P\leq0.05$, and $^{(*)}$ $0.05<P\leq0.1$ when compared with WT.

doi:10.1371/journal.pone.0113417.g003

Through the sequential fitting the relationship between [Pi] and ($2\pi b$+$2\pi c$) to Eq. 2, and relationship between [Pi] and tension to Eq. 3, the kinetic constants surrounding step 4 (k_4 and k_{-4}) and step 5 (K_5) as well as the force per cross-bridge (T_{56}) were deduced (Fig. 3C–E). Here K_5 is defined as the Pi association constant, and its dissociation constant is $1/K_5$. Despite the slightly decreased k_4 in t/t and significantly increased k_4 in SAS (Fig. 3E), there was no significant change found in K_4 in t/t and SAS (Fig. 3D). In contrast, in DAD, the slightly elevated k_4 and the slightly reduced k_{-4} (Fig. 3E) resulted in a significant increase in K_4 (Fig. 3D). K_5 was significantly decreased in t/t (Fig. 3D), indicating the Pi release was enhanced in the t/t mouse model. Both t/t and DAD mice displayed significantly smaller T_{56}, indicating the smaller force production per cross-bridge (Fig. 3C). Previously, tension with the standard activation (8 mM Pi) in t/t was less than that of WT, but their difference was insignificant (Fig. 3 of [17]). With the increased number of the Pi points between 0 mM and 30 mM, and fitting all

the data points available (n=168), we now conclude that force/cross-bridge (T_{56}) is less in t/t than in WT, and this difference is significant.

3. The ADP release step (step 0 in Fig. 1)

In contrast to the findings in the ATP study, the rate constant $2\pi c$ decreased and the tension increased as [ADP] increased in all groups of muscle fibres in the ADP study (Fig. 4A–B). t/t exhibited significantly smaller $2\pi c$ than that of WT at 00D ($P \leq 0.01$), $0D$ ($P \leq 0.05$) and 3D ($P \leq 0.05$), whereas DAD showed unaltered $2\pi c$. On the other hand, SAS exhibited a larger value of $2\pi c$ than WT at 1D ($P \leq 0.01$). The active tension was significantly less in DAD ($P \leq 0.01$ at all ADP concentration) and t/t ($P \leq 0.05$ at 1D and 2D, $P = 0.056$ at 3D) than that of WT mice (Fig. 4B). t/t and SAS displayed significantly smaller K_0, whereas ADA and DAD exhibited larger K_0 than that of WT (Fig. 4C). Here K_0 is defined as the ADP association constant, and its dissociation constant is $1/K_0$.

In the $00D$ solution, the rate constant $2\pi c$ was larger (Fig. 4A), and tension was less (Fig. 4B) than those in the 0D solution, demonstrating that the contaminating [ADP] in the 0D–3D solutions is significant. The contaminating ADP concentration (D_0) in the 0D–3D solutions, which resulted from ATP hydrolysis by muscle fibres and from ADP contamination present in ATP, was evaluated by extrapolating the $2\pi c$ data versus [ADP] (Fig. 4A, continuous curves) to the value of $2\pi c$ obtained in the 00D solution. The corresponding abscissa value is $-D_0$. We found that D_0 (in mM) was 0.44 ± 0.10 in WT ($n=12$), 0.71 ± 0.24 in t/t ($n=19$), 0.26 ± 0.06 in ADA ($n=12$), 0.35 ± 0.06 in DAD ($n=10$), and 0.26 ± 0.05 in SAS ($n=8$). Thus, 0.3–0.7 mM extra ADP was present in the 0D–3D solutions which do not have the ATP regenerating system. This extra ADP was taken into consideration when calculating K_0, as shown in Eq. 1.

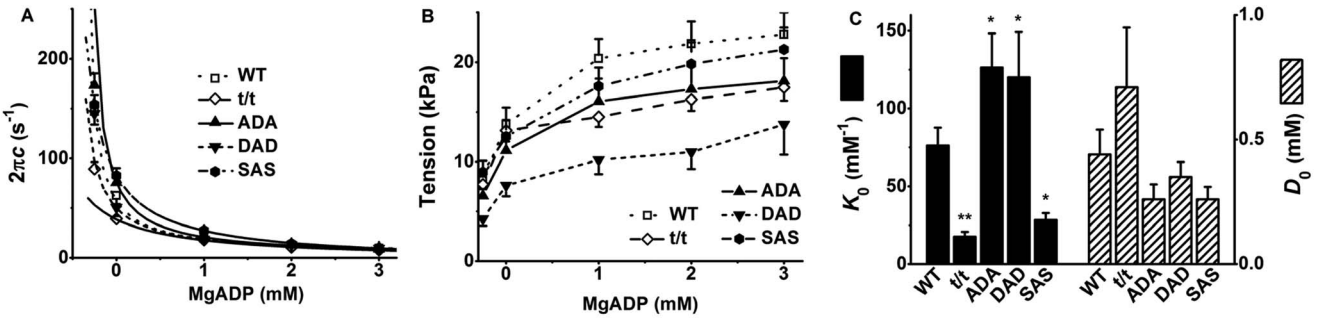

Figure 4. Results of the ADP study and parameters deduced from it. (A) $2\pi c$ versus [ADP] plot, (B) tension versus [ADP] plot, and (C) the ADP association constant (K_0) and ADP contamination (D_0). $n=12$, 19, 12, 10, and 8 for WT, t/t, ADA, DAD, and SAS mice, respectively. The continuous lines in (A) are the best fit curves to Eq. 1. $^{**}P \leq 0.01$ and $^{*}0.01 < P \leq 0.05$ when compared with WT.

doi:10.1371/journal.pone.0113417.g004

4. Cross-bridge distributions

To determine the number of force generating cross-bridges, the cross-bridge distribution was calculated among the AMDP, AM*DP, and AM*D states (Fig. 5). AMDP isomerizes to form AM*DP state and force is generated during this isomerization step [22,23,27,28], hence, AM*DP is a strongly attached state. The force generation (step 4) is followed by Pi release (step 5) to form the AM*D state, which maintains the same amount of force as the AM*DP state. Because of this, the distributions at AM*DP and AM*D are summated together and included in Fig. 5 to represent the number of strongly attached cross-bridges. t/t and DAD had more cross-bridge distributions than WT at the strongly attached state. ADA and SAS had no significant changes from WT in any of the states we observed (Fig. 5).

5. Rigor stiffness

To determine the strength of the actomyosin interaction and its associated change with the cMyBP-C mutants, rigor stiffness was measured and plotted in Fig. 6. The rigor stiffness is highly significantly decreased in t/t and DAD ($P \leq 0.01$), and significantly decreased in ADA ($P \leq 0.05$) compared to WT (Fig. 6).

6. Myofilament protein phosphorylation levels

To find out the influence of cMyBP-C mutations on phosphorylation of other myofilament proteins as well as cMyBP-C itself, cardiac muscle tissues were subjected to Pro-Q Diamond staining first, followed by SYPRO-Ruby staining. The representative gel from Pro-Q staining for phosphorylated protein and SYPRO-Ruby staining for total protein is shown in Fig. 7. The band densities were

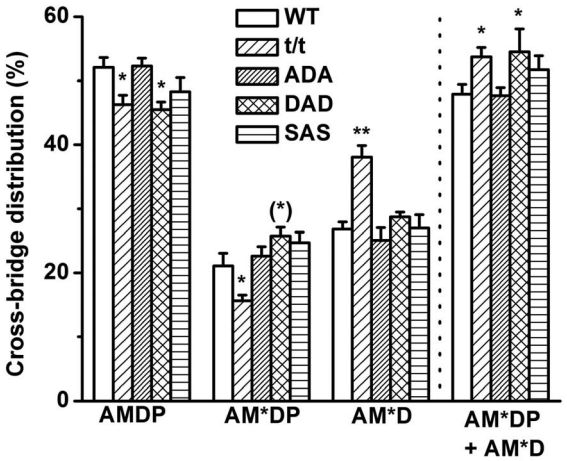

Figure 5. The cross-bridge distribution at the standard activating condition (*S*=5 mM and *P*=8 mM) among the AMDP, AM*DP, and AM*D states. **$P \leq 0.01$, *$0.01 < P \leq 0.05$, and (*) $0.05 < P \leq 0.1$ when compared with WT. AM*DP+AM*D indicate the total strongly attached cross-bridges.

doi:10.1371/journal.pone.0113417.g005

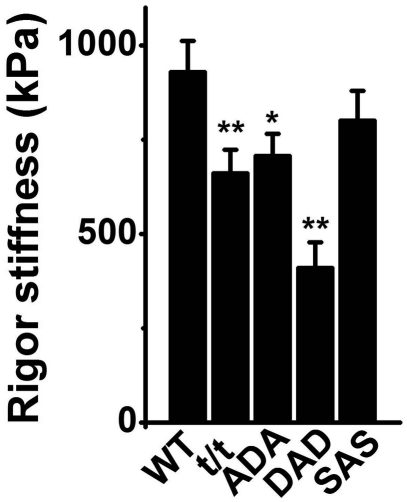

Figure 6. Rigor stiffness measured at 100 Hz. $^{**}P \leq 0.01$ and $^{*}0.01 < P \leq 0.05$ when compared with WT.

doi:10.1371/journal.pone.0113417.g006

calculated using Image-J software, and the relative phosphorylation levels of cMyBP-C, RLC, cTnI, cTnT, and Tm proteins are plotted in Fig. 8. The band of cMyBP-C was missing in t/t mouse from either Pro-Q Diamond or SYPRO-Ruby staining due to the cMyBP-C null genotype (Figs. 7 and 8A). The phosphorylation level of cMyBP-C was slightly decreased in ADA and DAD, but not changed in SAS compared to WT (Fig. 8A). The phosphorylation level of RLC was significantly decreased in t/t and ADA, slightly decreased in DAD, but not changed in SAS compared to WT (Fig. 8B). The phosphorylation levels of cTnI,

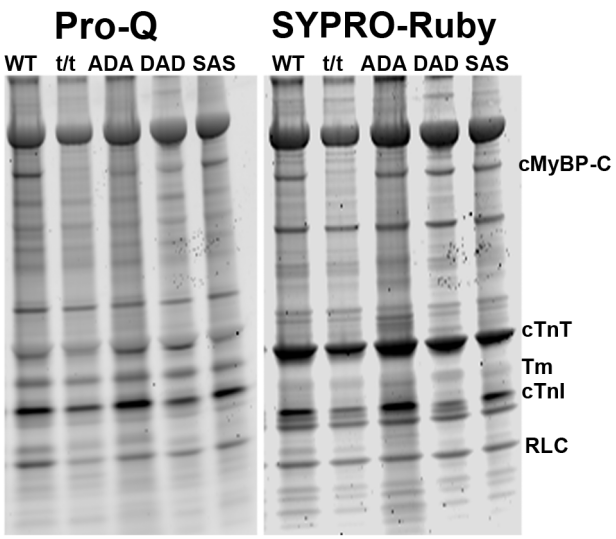

Figure 7. The representative gel of Pro-Q Diamond staining (*left*, phosphorylation) and SYPRO-Ruby staining (*right*, total protein).

doi:10.1371/journal.pone.0113417.g007

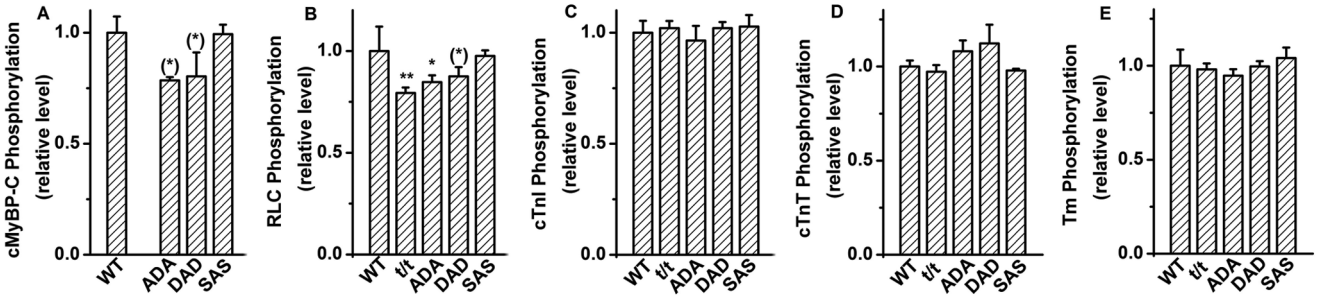

Figure 8. Protein phosphorylation level. (A) cMyBP-C, (B) RLC, (C) cTnI, (D) cTnT, and (E) Tm. $^{**}P \leq 0.01$, $^{*}0.01 < P \leq 0.05$, and $^{(*)}$ $0.05 < P \leq 0.1$ when compared with WT.

doi:10.1371/journal.pone.0113417.g008

cTnT and Tm (Fig. 8C–D) were not significantly different among all transgenic mouse models studied. In our study, muscle samples from WT and mutated mice were processed at the same time with the same procedures for comparability. We have shown that the phosphorylation levels do not change with time in skinned fibers, as we have demonstrated over the 8 month period (Fig. 3 of [29]).

Discussion

The present project aimed at finding the function of cMyBP-C phosphorylation in cardiac contractile mechanisms through characterizing the elementary steps of the cross-bridge cycle in cMyBP-C's phosphorylation site-mutated mice. Our study demonstrates that mutations of cMyBP-C's different phosphorylation site(s) differentially affect cross-bridge kinetics. Papillary muscle fibres from t/t mice showed the most broad effect with decreased force per cross-bridge (T_{56}, Fig. 3C), rigor stiffness (Fig. 6), cross-bridge detachment rate (k_2) (Fig. 2C), the ATP (K_1) (Fig. 2C), Pi (K_5, Fig. 3D), and ADP (K_0, Fig. 4C) association constants. DAD mice, carrying phospho-ablated S282 and phospho-mimetic S273 and S302 in cMyBP-C, had similar effects with t/t in decreased force per cross-bridge (T_{56}, Fig. 3C), decreased rigor stiffness (Fig. 6), decreased cross-bridge detachment rate (k_2, Fig. 2C), but had opposite changes from t/t in increased equilibrium constant of the force generation step (K_4, Fig. 3D), the increased ADP association step (K_0, Fig. 4C) without influencing the ATP binding (K_1, Fig. 2C) or Pi release step (K_5, Fig. 3D). ADA (phospho-mimetic S282 with phospho-ablated S273 and S302) mice showed decreased rigor stiffness (Fig. 6), increased ADP association (Fig. 4C), and the slightly increased ATP association (K_1) and the slightly increased cross-bridge detachment rate (k_2) (Fig. 2C). SAS (phospho-ablated S282) mice showed the decreased ATP (Fig. 2C) and ADP (Fig. 4C) association constants.

It has been observed that homozygous t/t mutant mice exhibited left ventricular dilation and reduced contractile function at birth, and progressed to a dilated cardiomyopathy with the reduced ejection fraction and maximal left ventricular end-systolic elastance, despite a preserved maximal rate of pressure rise; the

myocardial hypertrophy also increased as animals matured [30]. All ADA, DAD, and SAS mice have significantly increased interventricular septal thickness, increased left ventricular end-diastolic and end systolic dimensions, and variable extent of reduced fractional shortening [13]. Cardiac hypertrophy with fibrosis and myocyte disarray was observed in t/t and DAD mice [13]. In the present study, we found that t/t has the most profound effects and affected every elementary step involved in the cross-bridge cycle, hence the contractility represented by active tension, stiffness, and force per cross-bridge is significantly affected. In contrast, ADA, DAD, and SAS affected only limited steps in the cross-bridge cycle. These observations are consistent with the previous finding that the ADA, DAD and SAS partially rescued t/t phenotype [13]. However, the similar changes between t/t and DAD in tension, the apparent rate constant $2\pi c$ and the sum ($2\pi b$+$2\pi c$), and the rate constant of the cross-bridge detachment step (k_2) suggest that the DAD mice mimic the t/t mice in many mechanical profiles. The significantly smaller T_{56} (force produced/supported by each cross-bridge, Fig. 3C) is the reason for the decreased tension production in t/t and DAD, since the number of strongly attached cross-bridges at [AM*DP] and [AM*D] is larger in t/t and DAD mice than those in WT mice (Fig. 5). The similarly decreased force per cross-bridge in DAD and t/t mutants reinforces our previous conclusion that the protein kinase C (PKC) mediated S273 and S302 phosphorylation adversely affects the cross-bridge cycle and cardiac contraction [13].

Significantly decreased rate constant $2\pi c$ in the ATP and ADP studies (Figs. 2A and 4A, respectively) and decreased $2\pi b$+$2\pi c$ in the Pi study (Fig. 3A) were found in t/t in the present study. DAD mice showed similar changes (smaller $2\pi c$ and $2\pi b$+$2\pi c$; Figs. 2A, 3A, and 4A). These observations do not mean, however, that $2\pi b$ decreases in t/t and DAD mice: because $2\pi b$ is much smaller than $2\pi c$ ($2\pi c$ is 2–4 times of $2\pi b$), their sum (in the Pi study) is mostly governed by $2\pi c$. In fact, in the previous study, we found an increased rate constant $2\pi b$ and a decreased rate constant $2\pi c$ in DAD with the standard activation (see Fig. 4A of [17]), which made us to hypothesize that the cross-bridge detachment step(s) was decelerated, and/or the cross-bridge attachment step(s) was accelerated to result in a larger number of strongly attached cross-bridges with PKC sites (S273 and S302) phosphorylation. Our current finding, that k_2 (rate constant of cross-bridge detachment) is significantly less and K_4 (equilibrium constant of cross-bridge attachment/force generation step) is significantly more in DAD than WT (Figs. 2C and 3C), are in accord with our earlier hypothesis, which is also demonstrated in Fig. 5 that the number of strongly attached cross-bridges are more in DAD than in WT.

DAD shows some different effects from t/t: all ligand association constants (K_0, K_1, and K_5) are larger in DAD than those of t/t (Figs. 2C, 3D, and 4C). These effects indicate that the presence of cMyBP-C and its phosphorylation status significantly affect the nucleotide and Pi binding sites of myosin, indicating that there is a direct contact between cMyBP-C and the myosin head, or the signal is transmitted from the cMyBP-C binding site through the lever arm to the myosin head. The significantly larger K_4 in DAD than in t/t (Fig. 3D) contributes to the

transition of AMDP (weak) to AM*DP (strong) and causes more cross-bridges at the AM*DP state than in WT, and as shown in Fig. 5. The increased K_5 in DAD compared to t/t suggests that the Pi release decreases, causing less cross-bridges to transform from AM*DP to AM*D, a fact that can be seen as an inversion of the cross-bridge distributions in the AM*D state (Fig. 5). In all, we conclude that a large (~50%) tension and stiffness decrease in DAD is primarily due to a decrease in force per cross-ridge (Fig. 3), and the small increase in the number of strongly attached cross-bridges cannot compensate for this decrease (Fig. 5).

While t/t and DAD have large effects on tension and cross-bridge kinetics, the effects induced by ADA and SAS are small. In ADA, S273 and S302 are phospho-ablated, and in SAS the phosphorylation of S273 and S302 are strongly inhibited due to the phospho-ablated S282. S282 phosphorylation has been shown to play a leading role in the phosphorylation of other sites [10,13]. In ADA, with phospho-mimetic S282 and phospho-ablated S273 and S302, the significantly increased association constant for ADP (K_0, Fig. 4C) causes a reduced ADP release resulting in a slower sarcomere shortening. This is because the shortening velocity is controlled by the rate at which ADP can escape from cross-bridges after completion of the power stroke [31]. There is a strong correlation between the maximum ATP hydrolysis rate (V_{max}) and the rate of ADP release from actomyosin [32]. These observations may account for the reduced systolic function found in ADA mice [13]. In SAS with phospho-ablated S282, the result is opposite to ADA, as shown by the decreased K_0 and K_1 (Fig. 4C and 2C). No apparent abnormalities: fibrosis, calcification, or disarray, were found in the ADA or SAS mouse phenotype [13]. Therefore, the results in muscle mechanics in the present study and the histological results [13] are consistent. ADA and SAS produced small effects in cross-bridge kinetics with the only effects in K_0 and K_1; the increase in k_4 in SAS did not result in a significant change in K_4. The fact that ADA and SAS affect the ATP binding and ADP release steps, and DAD affects multiple steps demonstrates that a different mutant affects different elementary steps in the cross-bridge cycle. We have further found that t/t and DAD are more harmful mutations to cause detrimental effects than ADA and SAS mutations.

The fact that only central 9/17 (53%, c-zone) of the thick filament accompanies cMyBP-C, and the remaining 8/17 (47%, b-zone for cMyBP-C "bare" zone) does not accompany cMyBP-C [33] needs a consideration. Because cross-bridges in the two zones are mechanically in parallel, their total force (F, measured force) is the weighted sum of individual forces (F_c and F_b, respectively, which are force per unit length of the thick filament):

$$F = \frac{9}{17}F_c + \frac{8}{17}F_b \tag{4}$$

Where F_c is force if all the cross-bridges are accompanied with cMyBP-C, and F_b is force if none of the cross-bridges are accompanied with cMyBP-C. F_c and F change with a mutant, whereas F_b does not and it can be measured by the force t/t generates. From Eq. 4, we get:

$$F_c = \frac{17F - 8F_b}{9} \quad (5)$$

$$\text{From the t/t data, } F_b = F_{t/t} = 10.9 \pm 0.5 \text{ kPa } (N = 62) \quad (6)$$

The values for F is taken from averaged results of Figs. 2B and 3B at 5 mM MgATP and 8 mM Pi (standard activation).

$$\text{From Eqs. 5 and 6, } F_{c(WT)} = \frac{17(14.8 \pm 0.8kPa) - 8F_b}{9} = 18.2 \pm 1.6 \text{ kPa } (N = 37)$$

$$\text{Similarly, } F_{c(DAD)} = \frac{17(9.4 \pm 1.2kPa) - 8F_b}{9} = 8.2 \pm 2.2 \text{ kPa } (N = 26)$$

Thus, this analysis demonstrates that a cross-bridge with cMyBP-C generates (1.67 ± 0.10) fold ($=F_{c(WT)}/F_b = 18.2/10.9$) force compared to that without cMyBP-C. It further demonstrates that a cross-bridge with DAD mutant generates (0.45 ± 0.12) fold ($=F_{c(DAD)}/F_{c(WT)} = 8.2/18.2$) force compared to WT. Similar analysis demonstrates that a cross-bridge with ADA generates (0.86 ± 0.15) fold force ($F = 13.4 \pm 1.2$ kPa, $F_c = 15.6 \pm 2.2$ kPa, $N = 35$), SAS generates (1.02 ± 0.17) fold force ($F = 14.9 \pm 1.3$ kPa, $F_c = 18.5 \pm 2.5$ kPa, $N = 27$), and t/t generates (0.60 ± 0.06) fold force ($F = F_c = 10.9 \pm 0.5$ kPa, $N = 28$) compared to WT.

Previous works have shown that the phosphorylation of cMyBP-C disrupts its interaction with myosin S2, and causes a reduction in the distance between S1 and actin. This reduction may increase the probability of cross-bridge formation, and may accelerate the force generation step (see review by [34]). Our study has demonstrated that phosphorylation of the two PKC sites (Ser273 and Ser302) strengthens the interaction between cMyBP-C and myosin S2, but diminishes its interaction with actin [35]. However, the differential effects of each phosphorylation site on binding to S2 are not completely understood. These molecular interactions between cMyBP-C, myosin S2, and actin must be the bases for cMyBP-C induced active force enhancement as we observed in WT *vs.* t/t. One likely explanation is an allosteric activation of myosin so that it interacts with actin in a more efficient way. This interaction can be modulated by phosphorylation of cMyBP-C by a variety of protein kinases. Therefore, it can be concluded that the purpose of cMyBP-C is to increase the active force, and cMyBP-C's phosphorylation is to modulate the amount of active force generation depending on which protein kinase is activated in cardiomyocytes at a particular moment.

The phosphorylation status of cMyBP-C or its mutants may interfere with phosphorylation of other myofilament proteins. Our results indicate that the decreased or absence of cMyBP-C phosphorylation is accompanied with a decreased RLC phosphorylation (in t/t, ADA and DAD) (Fig. 8), suggesting that the phosphorylation of the two proteins is inter-related. The proposed physical interaction between the M-domain of cMyBP-C and RLC [36] may contribute to the RLC phosphorylation triggered by cMyBP-C phosphorylation. The close

correlation between cMyBP-C and RLC was also demonstrated in solution that cMyBP-C induced a significant increase in the actin-activated ATPase activity of both native and RLC-reconstituted myosin, but had no effect on RLC-deficient myosin [37]. The decreased RLC phosphorylation has no relation with the decreased tension per cross-bridge, because the latter only occurs in t/t and DAD, but not in ADA. However, we found that the rigor stiffness decreased in the t/t, ADA and DAD mice, all exhibited decreased RLC phosphorylation. Considering the influence of RLC phosphorylation on lever-arm stiffness [38], we conclude that the decreased RLC phosphorylation causes increased rigor stiffness, and this may be related to the altered distance of the myosin head to the thick filament [39]. A slightly decreased level of cMyBP-C phosphorylation was found in ADA [16], which is similar to our finding (Fig. 8).

A novel phosphorylation site Ser133 within the proline-alanine-rich linker domain between domains C0 and C1 was newly identified in human cMyBP-C [40]. This site could be phosphorylated by glycogen synthase kinase 3 beta (GSK3β), but not by protein kinase A (PKA). GSK3β has a modulating effect on sarcomere function by increasing the rate of tension redevelopment [40]. There is a possibility that additional phosphorylation sites in cMyBP-C may continue to be found, and its phosphorylation status may be associated with the phosphorylation of other sites.

The significantly decreased phosphorylation in cTnI, cTnT, RLC, and desmin, but not in cMyBP-C, was discovered in a study with frame shift mutation of cMyBP-C that was carried by hypertrophic cardiomyopathy patients [41]. In our mouse models, cMyBP-C protein was totally missing in the t/t mice and the mutated cMyBP-C was present at the similar levels in ADA, DAD, SAS, and WT mice (Fig. 7). This difference may cause a distinct effect on other myofilament proteins. An expression of skeletal TnT was found in the homozygous cardiac cMyBP-C-null (t/t) mice [42]. Specific antibody or mRNA probes are needed to identify these protein isoforms.

Several studies found that an increase in β-MHC expression in t/t mouse hearts [17,43–45], which may affect observed rate constants [46]. Consequently, our observations may be confounded by a mutation and an isoform shift. For this reason, we studied the MHC isoform content in our previous work [17]. We found that our conclusions on ADA, DAD, and SAS were not significantly affected, because the isoform shift in them were small. In t/t, there was a significant increase in β-MHC expression. However, the involvement of isoform shift may not modify our conclusions on tension, stiffness, or magnitude parameters, because tension is not sensitive to the MHC isoform shifting [46–48], and stiffness and magnitude parameters are generally scaled with tension. The decreased force/cross-bridge (T_{56}) in t/t is consistent with the observation that a partial ($29 \pm 3\%$) extraction of cMyBP-C resulted in ~30% reduction in maximal force [49].

The absence of cMyBP-C appear to cause a problem in cardiomyocyte organization, as demonstrated by disorganized and damaged sarcomere structures in t/t mice [13], which may cause further confounding problems. Consequently,

the ultrastructural changes may partly account for the decreased force/cross-bridge in this report. These problems are difficult to solve in fiber studies on transgenic mouse hearts, and additional methods with future experimentations are expected to sort them out.

Summary and Conclusions

DAD, similar to t/t, significantly reduces force per cross-bridge, apparent rate constant ($2\pi c$), and decelerates the cross-bridge detachment step. DAD mutant further demonstrates a reduced ADP release, and the elevated rate constant of the force generation step. These are different from t/t, which exhibited weakened ATP binding and enhanced Pi and ADP release. ADA and SAS mutants demonstrate insignificant impact on the force per cross-bridge, apparent rate constants, and the kinetics involved in steps 4–5. ADA slightly increases ATP binding and the cross-bridge detachment steps, and reduces ADP release, whereas SAS reduces ATP binding and promotes ADP release. Based on these findings, we conclude that the changes in the phosphorylation status of each site differentially affect the elementary steps of the cross-bridge cycle. In contrast to the limited influence on the ATP binding and the ADP release steps by ADA and SAS mutants, DAD produces broad effects by interfering with cross-bridge kinetics and negatively regulating force generation step, which largely mimic the t/t phenotype. Based on these findings, we conclude that it is the reduced force per cross-bridge, instead of the less numbers of strongly attached cross-bridges, that results in the reduced tension production in DAD and t/t mouse models. cMyBP-C, as an allosteric effector of myosin, increases the active force that cross-bridges generate, and its phosphorylation, which is regulated by variety of protein kinases, modulates the active force.

Author Contributions

Conceived and designed the experiments: LW SS MK. Performed the experiments: LW. Analyzed the data: LW SS MK. Contributed reagents/materials/analysis tools: LW SS MK. Wrote the paper: LW SS MK.

References

1. **Kawai M, Halvorson HR.** Force transients and minimum cross-bridge models in muscular contraction. J Muscle Res Cell Motil. 2007;28:371–395.
2. **Kawai M, Saeki Y, Zhao Y.** Crossbridge scheme and the kinetic constants of elementary steps deduced from chemically skinned papillary and trabecular muscles of the ferret. Circ Res. 1993;73:35–50.
3. **Offer G, Moos C, Starr R.** A new protein of the thick filaments of vertebrate skeletal myofibrils. Extractions, purification and characterization. J Mol Biol. 1973;74:653–676.
4. **Winegrad S.** Cardiac myosin binding protein C. Circ Res. 1999;84:1117–1126.
5. **Lim MS, Walsh MP.** Phosphorylation of skeletal and cardiac muscle C-proteins by the catalytic subunit of cAMP-dependent protein kinase. Biochem Cell Biol. 1986;64:622–630.

6. **Colson BA, Rybakova IN, Prochniewicz E, Moss RL, Thomas DD.** Cardiac myosin binding protein-C restricts intrafilament torsional dynamics of actin in a phosphorylation-dependent manner. Proc Natl Acad Sci U S A. 2012;109:20437–20442.

7. **Barefield D, Sadayappan S.** Phosphorylation and function of cardiac myosin binding protein-C in health and disease. J Mol Cell Cardiol. 2010;48:866–875.

8. **Michalek AJ, Howarth JW, Gulick J, Previs MJ, Robbins J, et al.** Phosphorylation modulates the mechanical stability of the cardiac myosin-binding protein C motif. Biophys J. 2013;104:442–452.

9. **Colson BA, Locher MR, Bekyarova T, Patel JR, Fitzsimons DP, et al.** Differential roles of regulatory light chain and myosin binding protein-C phosphorylations in the modulation of cardiac force development. J Physiol. 2010;588:981–993.

10. **Gautel M, Zuffardi O, Freiburg A, Labeit S.** Phosphorylation switches specific for the cardiac isoform of myosin binding protein-C: a modulator of cardiac contraction? Embo J. 1995;14:1952–1960.

11. **Yuan C, Guo Y, Ravi R, Przyklenk K, Shilkofski N, et al.** Myosin binding protein C is differentially phosphorylated upon myocardial stunning in canine and rat hearts– evidence for novel phosphorylation sites. Proteomics. 2006;6:4176–4186.

12. **Sadayappan S, de Tombe PP.** Cardiac myosin binding protein-C: redefining its structure and function. Biophys Rev. 2012;4:93–106.

13. **Sadayappan S, Gulick J, Osinska H, Barefield D, Cuello F, et al.** A critical function for Ser-282 in cardiac Myosin binding protein-C phosphorylation and cardiac function. Circ Res. 2011;109:141–150.

14. **Copeland O, Sadayappan S, Messer AE, Steinen GJ, van der Velden J, et al.** Analysis of cardiac myosin binding protein-C phosphorylation in human heart muscle. J Mol Cell Cardiol. 2010;49:1003–1011.

15. **Pearlman SM, Serber Z, Ferrell JE Jr.** A mechanism for the evolution of phosphorylation sites. Cell. 2011;147:934–946.

16. **Gupta MK, Gulick J, James J, Osinska H, Lorenz JN, et al.** Functional dissection of myosin binding protein C phosphorylation. J Mol Cell Cardiol. 2013;64C:39–50.

17. **Wang L, Ji X, Sadayappan S, M K.** Phosphorylation of cMyBP-C Affects Contractile Mechanisms in a Site-specific Manner. Biophys J. 2014;106:1112–1122.

18. **McConnell BK, Jones KA, Fatkin D, Arroyo LH, Lee RT, et al.** Dilated cardiomyopathy in homozygous myosin-binding protein-C mutant mice. J Clin Invest. 1999;104:1771.

19. **Wang L, Muthu P, Szczesna-Cordary D, Kawai M.** Diversity and similarity of motor function and cross-bridge kinetics in papillary muscles of transgenic mice carrying myosin regulatory light chain mutations D166V and R58Q. J Mol Cell Cardiol. 2013;62:153–163.

20. **Wang L, Muthu P, Szczesna-Cordary D, Kawai M.** Characterizations of myosin essential light chain's N-terminal truncation mutant Delta43 in transgenic mouse papillary muscles by using tension transients in response to sinusoidal length alterations. J Muscle Res Cell Motil. 2013;34:93–105.

21. **Kawai M, Brandt PW.** Sinusoidal analysis: a high resolution method for correlating biochemical reactions with physiological processes in activated skeletal muscles of rabbit, frog and crayfish. J Muscle Res Cell Motil. 1980;1:279–303.

22. **Kawai M, Halvorson HR.** Two step mechanism of phosphate release and the mechanism of force generation in chemically skinned fibers of rabbit psoas muscle. Biophys J. 1991;59:329–342.

23. **Kawai M, Zhao Y.** Cross-bridge scheme and force per cross-bridge state in skinned rabbit psoas muscle fibers. Biophys J. 1993;65:638–651.

24. **Zhao Y, Kawai M.** Kinetic and thermodynamic studies of the cross-bridge cycle in rabbit psoas muscle fibers. Biophys J. 1994;67:1655–1668.

25. **Steinberg TH, Agnew BJ, Gee KR, Leung WY, Goodman T, et al.** Global quantitative phosphoprotein analysis using Multiplexed Proteomics technology. Proteomics. 2003;3:1128–1144.

26. **Wang L, Muthu P, Szczesna-Cordary D, Kawai M.** Characterizations of myosin essential light chain's N-terminal truncation mutant Delta43 in transgenic mouse papillary muscles by using tension transients in response to sinusoidal length alterations. J Muscle Res Cell Motil. 2013.

27. **Dantzig JA, Goldman YE, Millar NC, Lacktis J, Homsher E.** Reversal of the cross-bridge force-generating transition by photogeneration of phosphate in rabbit psoas muscle fibres. J Physiol. 1992;451:247–278.

28. **Fortune NS, Geeves MA, Ranatunga KW.** Tension responses to rapid pressure release in glycerinated rabbit muscle fibers. Proc Natl Acad Sci U S A. 1991;88:7323–7327.

29. **Bai F, Wang L, Kawai M.** A study of tropomyosin's role in cardiac function and disease using thin-filament reconstituted myocardium. J Muscle Res Cell Motil. 2013;34:295–310.

30. **McConnell BK, Jones KA, Fatkin D, Arroyo LH, Lee RT, et al.** Dilated cardiomyopathy in homozygous myosin-binding protein-C mutant mice. J Clin Invest. 1999;104:1235–1244.

31. **Weiss S, Rossi R, Pellegrino MA, Bottinelli R, Geeves MA.** Differing ADP release rates from myosin heavy chain isoforms define the shortening velocity of skeletal muscle fibers. J Biol Chem. 2001;276:45902–45908.

32. **Siemankowski RF, Wiseman MO, White HD.** ADP dissociation from actomyosin subfragment 1 is sufficiently slow to limit the unloaded shortening velocity in vertebrate muscle. Proc Natl Acad Sci U S A. 1985;82:658–662.

33. **Luther PK, Bennett PM, Knupp C, Craig R, Padron R, et al.** Understanding the organisation and role of myosin binding protein C in normal striated muscle by comparison with MyBP-C knockout cardiac muscle. J Mol Biol. 2008;384:60–72.

34. **Granzier HL, Campbell KB.** New insights in the role of cardiac myosin binding protein C as a regulator of cardiac contractility. Circ Res. 2006;99:795–797.

35. **Govindan S, Mou Y, Lynch T, Tombe P, Sadayappan S.** Protein kinase C-site phosphorylation of cardiac myosin binding protein-C decreases cross-bridge kinetics. The FASEB Journal. 2014;28:S1081.1085.

36. **Pfuhl M, Gautel M.** Structure, interactions and function of the N-terminus of cardiac myosin binding protein C (MyBP-C): who does what, with what, and to whom? J Muscle Res Cell Motil. 2012;33:83–94.

37. **Margossian SS.** Reversible dissociation of dog cardiac myosin regulatory light chain 2 and its influence on ATP hydrolysis. J Biol Chem. 1985;260:13747–13754.

38. **Greenberg MJ, Mealy TR, Watt JD, Jones M, Szczesna-Cordary D, et al.** The molecular effects of skeletal muscle myosin regulatory light chain phosphorylation. Am J Physiol Regul Integr Comp Physiol. 2009;297:R265–274.

39. **Levine RJ, Yang Z, Epstein ND, Fananapazir L, Stull JT, et al.** Structural and functional responses of mammalian thick filaments to alterations in myosin regulatory light chains. J Struct Biol. 1998;122:149–161.

40. **Kuster DW, Sequeira V, Najafi A, Boontje NM, Wijnker PJ, et al.** GSK3beta phosphorylates newly identified site in the proline-alanine-rich region of cardiac myosin-binding protein C and alters cross-bridge cycling kinetics in human: short communication. Circ Res. 2013;112:633–639.

41. **van Dijk SJ, Dooijes D, dos Remedios C, Michels M, Lamers JM, et al.** Cardiac myosin-binding protein C mutations and hypertrophic cardiomyopathy: haploinsufficiency, deranged phosphorylation, and cardiomyocyte dysfunction. Circulation. 2009;119:1473–1483.

42. **Cazorla O, Szilagyi S, Vignier N, Salazar G, Kramer E, et al.** Length and protein kinase A modulations of myocytes in cardiac myosin binding protein C-deficient mice. Cardiovasc Res. 2006;69:370–380.

43. **Sadayappan S, Gulick J, Osinska H, Martin LA, Hahn HS, et al.** Cardiac myosin-binding protein-C phosphorylation and cardiac function. Circ Res. 2005;97:1156–1163.

44. **Palmer BM, Sadayappan S, Wang Y, Weith AE, Previs MJ, et al.** Roles for cardiac MyBP-C in maintaining myofilament lattice rigidity and prolonging myosin cross-bridge lifetime. Biophys J. 2011;101:1661–1669.

45. **Desjardins CL, Chen Y, Coulton AT, Hoit BD, Yu X, et al.** Cardiac myosin binding protein C insufficiency leads to early onset of mechanical dysfunction. Circ Cardiovasc Imaging. 2012;5:127–136.

46. **Wang Y, Tanner BC, Lombardo AT, Tremble SM, Maughan DW, et al.** Cardiac myosin isoforms exhibit differential rates of MgADP release and MgATP binding detected by myocardial viscoelasticity. J Mol Cell Cardiol. 2013;54:1–8.

47. **Mamidi R, Chandra M.** Divergent effects of alpha- and beta-myosin heavy chain isoforms on the N terminus of rat cardiac troponin T. J Gen Physiol. 2013;142:413–423.

48. **Rundell VL, Manaves V, Martin AF, de Tombe PP.** Impact of beta-myosin heavy chain isoform expression on cross-bridge cycling kinetics. Am J Physiol Heart Circ Physiol. 2005;288:H896–903.

49. **Kulikovskaya I, McClellan G, Levine R, Winegrad S.** Effect of extraction of myosin binding protein C on contractility of rat heart. Am J Physiol Heart Circ Physiol. 2003;285:H857–865.